Journal of Breast Cancer

J Breast Cancer 2018 June; 21(2): 103-111 https://doi.org/10.4048/jbc.2018.21.2.103

Check for updates

ORIGINAL ARTICLE

Knockdown of Chloride Channel-3 Inhibits Breast Cancer Growth *In Vitro* and *In Vivo*

Fang-Min Zhou[1,*], Yun-Ying Huang[1,2,*], Tian Tian[1], Xiao-Yan Li[3], Yong-Bo Tang[1]

[1]Department of Pharmacology, Zhongshan School of Medicine, Sun Yat-sen University, Guangzhou; [2]Department of Pharmacy, The Fifth Affiliated Hospital of Guangzhou Medical University, Guangzhou; [3]Department of Clinical Pharmacology, The Sixth Affiliated Hospital of Sun Yat-sen University, Guangzhou, China

Purpose: Chloride channel-3 (ClC-3) is a member of the chloride channel family and plays a critical role in a variety of cellular activities. The aim of the present study is to explore the molecular mechanisms underlying the antitumor effect of silencing ClC-3 in breast cancer. **Methods:** Human breast cancer cell lines MDA-MB-231 and MCF-7 were used in the experiments. Messenger RNA and protein expression were examined by quantitative real-time polymerase chain reaction and western blot analysis. Cell proliferation was measured by the bromodeoxyuridine method, and the cell cycle was evaluated using fluorescence-activated cell sorting. Protein interaction in cells was analyzed by co-immunoprecipitation. Tumor tissues were stained with hematoxylin-eosin and tumor burden was measured using the Metamorph software. **Results:** Breast cancer tissues collected from patients showed an increase in ClC-3 expression. Knockdown of ClC-3 inhibited the secretion of insulin-like growth factor (IGF)-1, cell proliferation, and G1/S transition in breast cancer cells. In the mouse xenograft model of human breast carcinoma, tumor growth was significantly slower in animals injected with ClC-3-deficient cells compared with the growth of normal human breast cancer cells. In addition, silencing of ClC-3 attenuated the expression of proliferating cell nuclear antigen, Ki-67, cyclin D1, and cyclin E, as well as the activation of extracellular signal-regulated protein kinases (ERK) 1/2, both *in vitro* and *in vivo*. **Conclusion:** Together, our data suggest that upregulation of ClC-3 by IGF-1 contributes to cell proliferation and tumor growth in breast cancer, and ClC-3 deficiency suppresses cell proliferation and tumor growth via the IGF/IGF receptor/ERK pathway.

Key Words: *Breast neoplasms, Cell proliferation, Chloride channel-3, Insulin-like growth factor 1*

INTRODUCTION

Breast cancer is the most common invasive cancer in women, comprising approximately 23% of all female cancers worldwide [1,2]. Although effective treatment methods including surgery, radiation therapy, and chemotherapy exist, breast cancer frequently shows poor response to these therapies. Therefore, researchers must gain a better understanding of the mechanisms underlying the development of breast cancer to identify highly effective drugs that lead to better outcomes for breast cancer patients.

Recent studies have demonstrated that chloride channel-3 (ClC-3) is expressed in breast cancer [3], cervical cancer [4], prostate cancer [5], nasopharyngeal cancer [6], osteosarcoma [7], leukemia [8], and glioma tumors [9], and its expression increases with tumor progression. The functions of ClC-3 are associated with the pathophysiology and progression of tumors. These include cell cycle regulation, cell proliferation, migration, and apoptosis in many cancers [10,11]. In our previous investigation, using flow cytometric assays, we found that silencing of ClC-3 caused cell cycle arrest in the G0/G1 phase and inhibition of cell proliferation [12]. However, downregulation of ClC-3 expression by treatment with antisense oligonucleotides arrested the cell cycle in the S phase in vascular smooth muscle cells [13]. The aim of the present

Correspondence to: Yong-Bo Tang
Department of Pharmacology, Zhongshan School of Medicine, Sun Yat-sen University, 74 Zhongshan 2 Road, Guangzhou 510080, China
Tel: +86-20-87331857, Fax: +86-20-87334740
E-mail: tangyb@mail.sysu.edu.cn

*These authors contributed equally to this work.

This work is supported by the National Natural Science Foundation of China (No. 81503063, No. 81573419), Natural Science Foundation of Guangdong Province (No. 2016A030310270, No. 2016A030313191, No. 2015A030313061), and Medical and Health Science and Technology Project of Guangzhou (No. 20161A011093).

Received: November 8, 2017 **Accepted:** May 4, 2018

http://ejbc.kr | pISSN 1738-6756
eISSN 2092-9900

study is to explore the molecular mechanisms underlying the antitumor effect of silencing ClC-3 in breast cancer.

METHODS

Quantitative real-time polymerase chain reaction

The present study was approved by the ethics committee of the Sun Yat-sen University (No. 2016-447XS) and adhered to the tenets of the Declaration of Helsinki. Additionally, written informed consent was obtained from the patients. Investigators are required to obtain informed consent before enrolling participants in clinical trials. The total RNA was isolated from human breast tissue using Trizol (Invitrogen, Carlsbad, USA). One microgram of total RNA was reverse-transcribed and used in SYBR Green real-time polymerase chain reaction (RT-PCR) as described previously [14]. Samples were run in triplicate with RNA preparation. QuantiTect primers are shown in Table 1. Quantitative RT-PCR (qRT-PCR) analyses were carried out on a MyiQ Single Color Real-time PCR Detection System (Bio-Rad Laboratories, Hercules, USA) for 40 cycles at 95°C for 15 seconds and 60°C for 1 minute, after an initial incubation at 95°C for 2 minutes. The fold change in messenger RNA (mRNA) expression of target genes was calculated using the $2^{-\Delta\Delta CT}$ method with glyceraldehyde 3-phosphate dehydrogenase as an internal control.

Cells and cell culture

Human breast cancer cell lines MDA-MB-231 and MCF-7 were cultured in Dulbecco's modified Eagle's medium (DMEM) with 10% fetal bovine serum at 37°C in 5% CO_2 [15].

Table 1. Primers used in the qRT-PCR assay for the elevated chloride channels

Gene name	RefSeq	Primer direction	Primer sequence
hClC-1	NM_000083.2	Sense	TGATATCCTGACGGTGGGCT
		Anti-sense	GTGTCCCAAAACAACAGCCG
hClC-2	NM_004366.5	Sense	ACTATGCCATTGCTGCCTGT
		Anti-sense	TGGAGCAAGATGCTGGTGTT
hClC-3	NM_173872.3	Sense	GACAATGTGTGGTTTGGCCT
		Anti-sense	CATATCGGCCTACACTGCGT
hClC-4	NM_001256944.1	Sense	CTGCAGGCACCTTGGCT
		Anti-sense	CCTTCAGGTCCGTCATCCAG
hClC-5	NM_001127899.3	Sense	GCTGCTCCAACCTCCTTTTTG
		Anti-sense	GAGTGGCTAAAGGCAGTGTGA
hClC-6	NM_001256959.1	Sense	AGGAAAGACTATGAGAAAGGTCG
		Anti-sense	GAGTTGGGTGAAGAGTCGCA
hClC-7	NM_001287.5	Sense	CTAAGAAGGTGTCCTGGTCCG
		Anti-sense	GGAAAAGCGCAGAACGTGG
hCFTR	NM_000492.3	Sense	ACTGGAGCAGGCAAGACTTC
		Anti-sense	TGGTGCCAGGCATAATCCAG

qRT-PCR = quantitative real-time polymerase chain reaction.

Transfection of MDA-MB-231 cells with stealth siRNA

The sequence of the stealth small interfering RNA (siRNA) duplex oligoribonucleotides against human voltage-gated channel 3 (RefSeq NM_173872.3) is 5′-UCACCAAGGAAACUGCAAGAAAGGC-3′, and its corresponding complementary strand is 5′-GCCUUUCUUGCAGUUUCCUUGGUGA-3′ (Life Technologies, Carlsbad, USA). ClC-3 siRNA was transfected into MDA-MB-231 cells transiently using Lipofectamine™ RNAiMAX (Invitrogen) in accordance with the manufacturer's instructions and a negative control stealth siRNA sequence was used.

Briefly, siRNA and Lipofectamine™ RNAiMAX reagent were diluted in Opti-MEMI Medium (Invitrogen). Then, the diluted siRNA and Lipofectamine™ RNAiMAX were mixed and incubated for 20 minutes at room temperature (15°C–25°C) to allow the formation of transfection complexes. Droplets of the complexes were added to the MDA-MB-231 cells while they were in quiescent state and all were swirled gently in order to ensure uniform distribution. After incubation for 8 hours at 37°C, the final transfection mixture was removed, and the MDA-MB-231 cells were incubated under normal growth conditions before conducting the experiments. BLOCK-iT Fluorescent Oligo (Thermo Fisher Scientific, Waltham, USA) and siRNA-labeled fluorescein isothiocyanate (Life Technologies) were used to determine the transfection efficiency.

Cell counting and incorporation of bromodeoxyuridine

Cell proliferation was measured by cell counting and by bromodeoxyuridine (BrdU) incorporation as previously described [12], using a BrdU kit (Calbiochem, San Diego, USA) in accordance with the manufacturer's instructions. After incubation, cells were mixed with 10 mmol/L BrdU for 18 hours, and DNA was denatured in a fixative/denaturing solution for 30 minutes to enable antibody binding to the incorporated BrdU. Then, anti-BrdU monoclonal antibody was incubated for 1 hour at room temperature. After washing, the samples were then treated with horseradish peroxidase (HRP)-conjugated goat anti-mouse immunoglobulin G for 30 minutes. Colorless 3,3′,5,5′-tetramethylbenzidine (100 mmol/L) was added as the substrate of HRP. The colored reaction product was quantified by measuring the optical density at 450–540 nm using a microplate reader.

Cell cycle analysis

Cells were seeded, treated, and then processed for cell cycle analysis using the propidium iodide staining method as previ-

https://doi.org/10.4048/jbc.2018.21.2.103

ously described [12]. Cells were analyzed for DNA content using flow cytometry. The percentage of cells containing different multiple strands of DNA was quantified.

Western blot and co-immunoprecipitation assay

Whole cell or tissues extracts were digested in radioimmunoprecipitation lysis buffer (Beyotime, Wuhan, China) containing 1 mM phenylmethylsulfonyl fluoride (Beyotime). Total proteins were isolated and quantified by bicinchoninic acid protein assay (Beyotime). The protein lysates (20 μg) were resolved by sodium dodecyl sulfate-polyacrylamide gel electrophoresis. The separated proteins were transferred onto polyvinylidene difluoride membranes and blocked at room phenylmethylsulfonyl temperature for 1 hour in Tris-buffered saline and Tween 20 with 5% nonfat dry milk. The membranes were incubated overnight at 4°C with the primary antibodies. Then, the membranes were incubated with HRP secondary antibodies (Abcam, Cambridge, UK) for 1 hour at room temperature, and the protein bands were detected with a ChemiDoc™ XRS+ and Image Lab™ software (Bio-Rad Laboratories). Cellular protein expression and phosphorylation were determined via western blot analysis as previously described [12]. Cultured MDA-MB-231 cells were harvested for co-immunoprecipitation (co-IP) as previously described [16].

Xenograft model and *in vivo* treatment

All animal experiments were approved by Sun Yat-sen University for animal research and performed in compliance with the National Institutes of Health Guide for the Care and Use of Laboratory Animals (issued by the Ministry of Science and Technology of China, Beijing). Female athymic BALB/c nude mice (4 weeks old) were purchased from Vital River Laboratories (Beijing, China). Short hairpin RNA (shRNA)-mediated ClC-3-deficient MDA-MB-231 cells were obtained as described in our previous study [15]. When the mice turned 5 weeks old, 3×10^6 shRNA-mediated ClC-3-deficient MDA-MB-231 cells and normal MDA-MB-231 breast cancer cells suspended in 100 μL of serum-free and antibiotic-free DMEM were injected subcutaneously into their flanks. Tumor dimensions were measured with a digital vernier caliper every 4 days and the tumor volume was calculated using the formula $\pi/6 \times (\text{length}) \times (\text{width})^2$. The day of inoculation was designated as day 0, and all mice in the study were sacrificed on day 20 postinoculation.

Histology and immunohistochemistry

Tumor tissues were embedded in paraffin and 4 μm-thick transverse sections were cut and stained with hematoxylin-eosin. To assess the tumor burden, the tumor area in each section was measured using Metamorph software (Universal Imaging Corp., Downington, USA). Cellular proliferation was evaluated by assessing the expression of Ki-67 (Cell Signaling Technology, Beverly, USA) in the tumor sections.

Statistical analysis

Unless otherwise indicated, values are presented as mean ± standard deviation and n represents the number of independent experiments. Comparisons between the two groups were

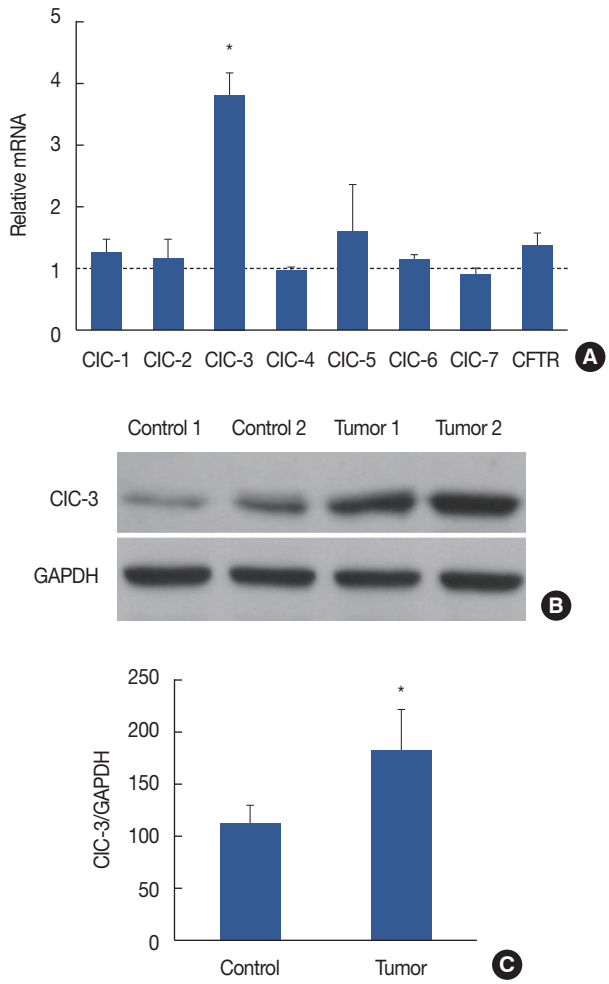

Figure 1. Chloride channel-3 (ClC-3) expression in breast tumor tissues. (A) Chloride channels (ClC-1–7, CFTR) are expressed in human breast cancer tissues from clinical postoperative patients, as indicated by qRT-PCR mRNA analysis. The data are presented as relative fold changes in breast cancer tissues versus normal tissues. (B) Expression of ClC-3 was examined by western blotting, (C) ClC-3 protein is expressed in breast cancer tissues. The result shows a significant increase in ClC-3 expression in breast cancer tissues vs. normal tissues.
CFTR = cystic fbrosis transmembrane conductance regulator; qRT-PCR = quantitative real-time polymerase chain reaction; mRNA = messenger RNA; GAPDH = glyceraldehyde 3-phosphate dehydrogenase. *$p < 0.01$ vs. control.

performed using the unpaired two-tailed Student t-test. For comparisons of three or more groups, analysis of variance and Bonferroni multiple-comparison post hoc test were employed using the SPSS system (IBM Corp., Armonk, USA). $p<0.05$ was considered statistically significant.

RESULTS

Human breast cancer tissues express chloride channels

The presence of mRNA encoding seven members of the chloride channel family and cystic fibrosis transmembrane conductance regulator (CFTR) in human breast cancer tissue was studied using qRT-PCR. qRT-PCR was performed using specific primers revealed through significant variations in expression among the different members of the chloride channel family and CFTR in human breast cancer tissues. As shown in Figure 1A, the order of relative abundance was ClC-3 (3.78±0.32), ClC-5 (1.56±0.63), CFTR (1.35±0.17), ClC-1 (1.21±0.21), ClC-2 (1.12±0.28), ClC-6 (1.08±0.12), ClC-4 (0.95±0.07), and ClC-7 (0.82±0.14). Thus, ClC-3 is the predominant member of the chloride channel family.

ClC-3 is overexpressed in breast tumor tissues compared to normal breast tissues

Figure 1B and 1C is a representative immunoblot analysis demonstrating ClC-3 expression in two of the six patients enrolled in this study. ClC-3 levels were significantly overexpressed in breast tumor tissues (upregulated by >50%, $p<0.01$) compared with their normal counterparts.

Insulin-like growth factor 1 upregulated ClC-3 expression in human breast cancer cells

ClC-3 has been found in the highly malignant human breast cancer cell lines MDA-MB-231 and MCF-7 [3]. However, it is unknown whether insulin-like growth factor 1 (IGF-1) affects the expression of ClC-3. As shown in Figure 2, western blotting indicated that the protein expression of ClC-3 was increased in MDA-MB-231 and MCF-7 cells incubated with IGF-1. When incubated with 30–300 ng/mL IGF-1 for up to 24 hours, ClC-3 protein expression was increased in a concentration-dependent manner. Exposure to IGF-1 (100 ng/mL) for 24 hours led to a 4-fold induction of ClC-3 protein expression compared with those that were treated with the substance alone ($p<0.01$). The additional experiments to detect the levels of IGF-1 expression by knockdown of ClC-3. The results reveal that IGF-1 was significantly decreased by knockdown of ClC-3 in secretion of MDA-MB-231 cells (Supplementary Figure 1, available online).

Knockdown of ClC-3 inhibits cell proliferation in human breast cancer cells

Uncontrolled cellular proliferation plays a key role in promoting breast cancer progression, so we investigated the effects of ClC-3 on the proliferation of MDA-MB-231 cells. Compared to the control group, 100 ng/mL IGF-1 led to 1.8±0.3-fold and 1.6±0.2-fold ($p<0.01$, n=5) increments in BrdU incorporation (Figure 3A) and cell number (Figure 3B), respectively. ClC-3 siRNA inhibited IGF-1-induced cell growth and BrdU incorporation by 82.6%±6.4% and 79%±5.7% in

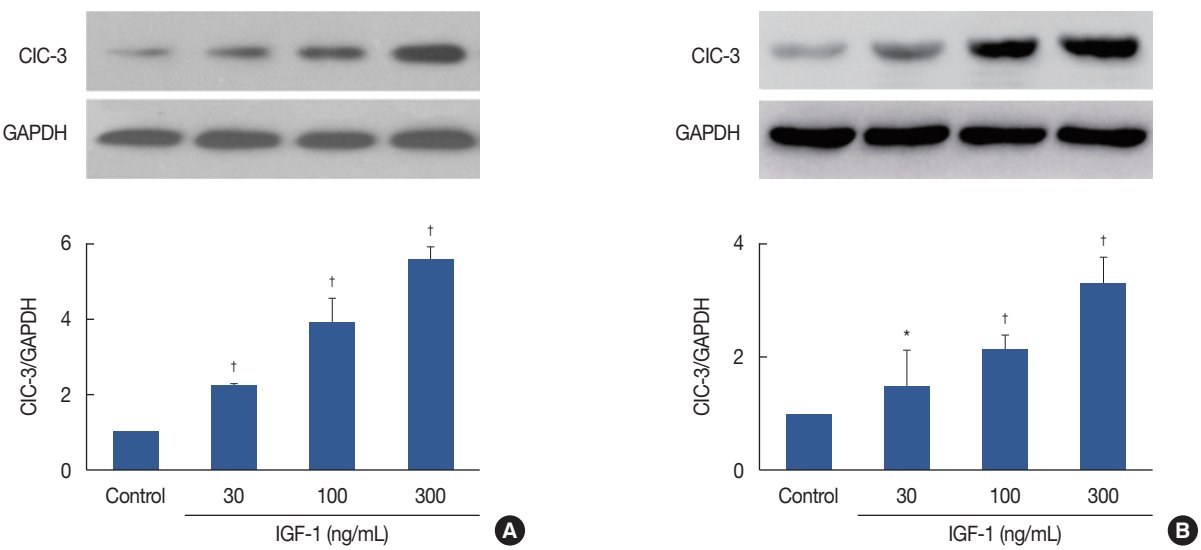

Figure 2. Insulin-like growth factor 1 (IGF-1) and chloride channel-3 (ClC-3) expression in human breast cancer cells. (A) Effect of 30–300 ng/mL IGF-1 on the expression of ClC-3 in MDA-MB-231 cells. (B) Effect of 30–300 ng/mL IGF-1 on the expression of ClC-3 in MCF-7 cells (n=5). GAPDH=glyceraldehyde 3-phosphate dehydrogenase. *$p<0.05$ vs. control; †$p<0.01$ vs. control.

https://doi.org/10.4048/jbc.2018.21.2.103

MDA-MB-231 cells, respectively, while negative siRNA had no significant effect on IGF-1-induced cell proliferation, excluding the nonspecificity of the siRNA and transfection reagent.

As shown in Figure 3C, serum-starved MDA-MB-231 cells in the control group were mostly in the G0/G1 (81.1%) and S phases (14.9%). After treatment with IGF-1, a decrease from 81.1% to 62.6% in the G0/G1 phase and an increase from 14.9% to 32.7% in the S phase ($p<0.01$, n=5) indicated that IGF-1 led to cell cycle progression, accelerating the transition from the G0/G1 to S phase. Treatment of MDA-MB-231 cells with ClC-3 siRNA resulted in an increased percentage of cell populations in the G0/G1 phase and a decreased percentage in the S phase (Figure 3C).

Effect of ClC-3 knockdown on cell cycle protein expression

We first analyzed the expression of two proliferation markers widely used in clinical studies, namely Ki-67 and proliferating cell nuclear antigen (PCNA) (Figure 4). The knockdown of ClC-3 inhibited proliferation in MDA-MB-231 cells compared to that in the control group, as measured by western blot analysis. To explore the mechanisms by which knockdown of ClC-3 arrests the cell cycle in the G0/G1 phase, we analyzed changes in proteins that regulate cell cycle progression, including cyclin D1, cyclin E, and cyclin dependent kinase (CDK) interacting protein 1 (p21). As shown in Figure 4, IGF-1 increased the expressions of cyclin D1 and cyclin E by 2.2±0.2 folds and 1.6±0.1 folds, respectively, and decreased the expressions of p21 by 70.9%±6.4% ($p<0.01$, n=5). The alterations induced by IGF-1 were completely reversed by the ClC-3 siRNA. The signal-responsive interaction of ClC-3 with IGF receptor (IGF-R) in IGF-1-treated cells induced extracellular signal-regulated protein kinases 1/2 (ERK1/2) activation.

The signal-responsive interaction of ClC-3 with IGF-R in IGF-1-induced ERK1/2 activation

We initially examined the ERK1/2 pathway to investigate events upstream to the IGF-1-induced cell proliferation. Cells

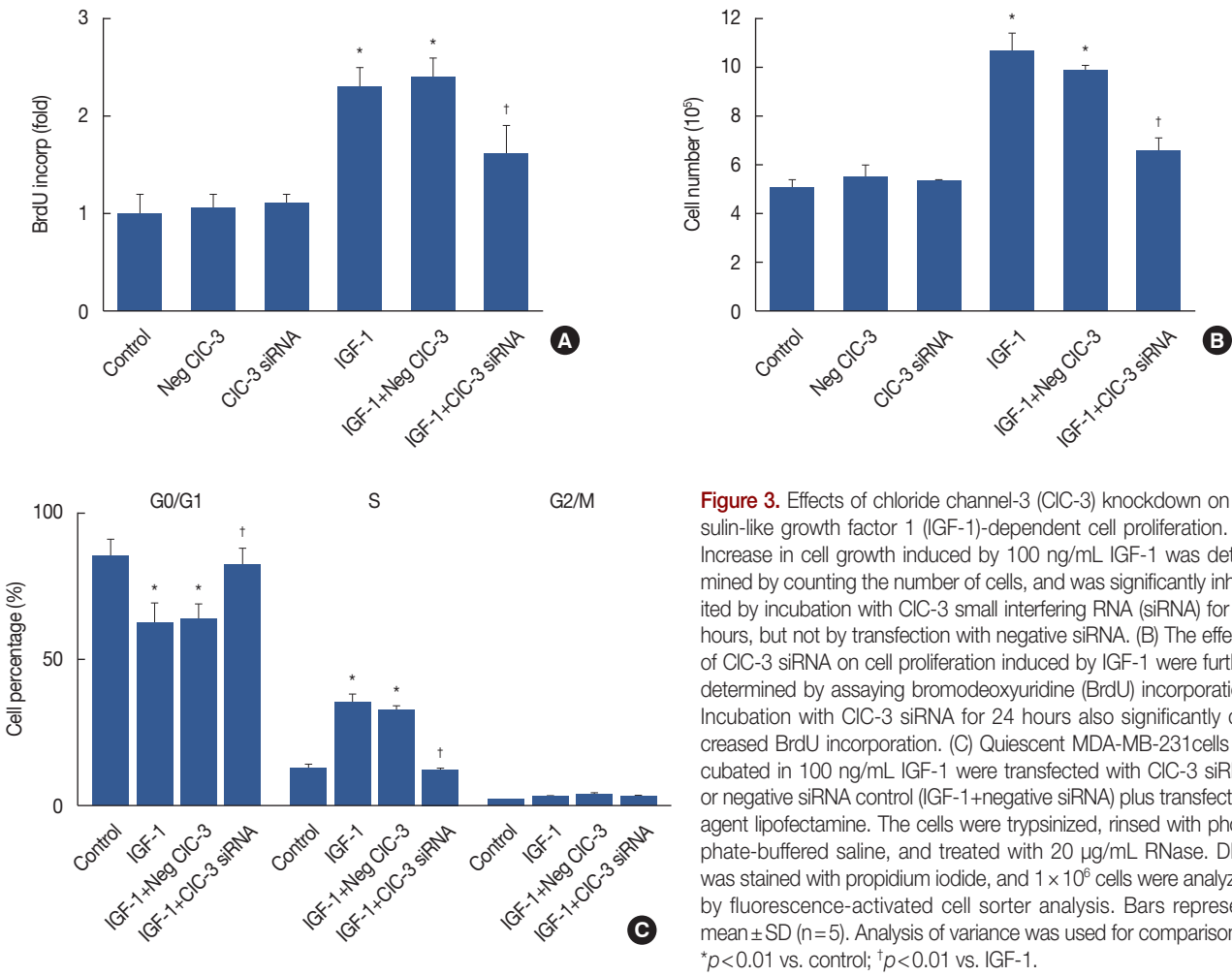

Figure 3. Effects of chloride channel-3 (ClC-3) knockdown on insulin-like growth factor 1 (IGF-1)-dependent cell proliferation. (A) Increase in cell growth induced by 100 ng/mL IGF-1 was determined by counting the number of cells, and was significantly inhibited by incubation with ClC-3 small interfering RNA (siRNA) for 24 hours, but not by transfection with negative siRNA. (B) The effects of ClC-3 siRNA on cell proliferation induced by IGF-1 were further determined by assaying bromodeoxyuridine (BrdU) incorporation. Incubation with ClC-3 siRNA for 24 hours also significantly decreased BrdU incorporation. (C) Quiescent MDA-MB-231cells incubated in 100 ng/mL IGF-1 were transfected with ClC-3 siRNA or negative siRNA control (IGF-1+negative siRNA) plus transfecting agent lipofectamine. The cells were trypsinized, rinsed with phosphate-buffered saline, and treated with 20 μg/mL RNase. DNA was stained with propidium iodide, and 1×10^6 cells were analyzed by fluorescence-activated cell sorter analysis. Bars represent mean±SD (n=5). Analysis of variance was used for comparison. *$p<0.01$ vs. control; †$p<0.01$ vs. IGF-1.

treated with IGF-1 were subjected to western blotting with antibodies that specifically recognize phosphorylated ERK1/2 (pERK1/2). Then, the cells were treated with ClC-3 shRNA to confirm whether the knockdown of ClC-3 led to inactivation of pERK1/2. IGF-1-induced activation of pERK1/2 was attenuated in the presence of ClC-3 shRNA (Figure 5A). To under-

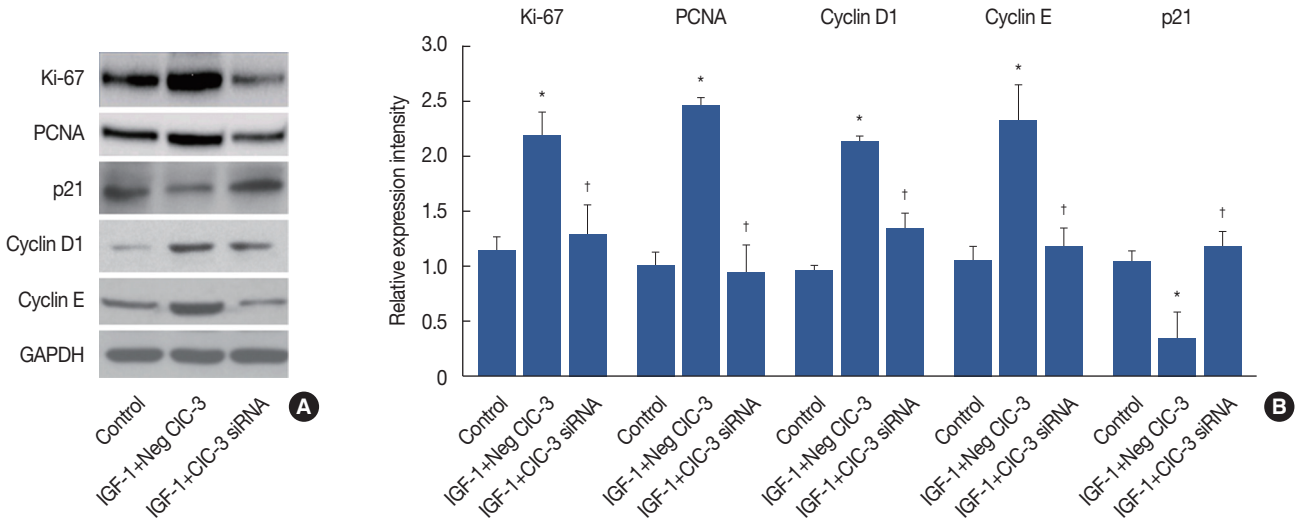

Figure 4. Effects of chloride channel-3 (ClC-3) knockdown on the expression of cell cycle-regulatory proteins. (A) Representative western blot images of Ki-67, proliferating cell nuclear antigen (PCNA), cyclins, and p21. (B) Densitometric analysis of the effects of ClC-3 knockdown on expression of Ki-67, PCNA, cyclin D1, cyclin E, and p21 (n=5).
GAPDH=glyceraldehyde 3-phosphate dehydrogenase; IGF-1=insulin-like growth factor 1; siRNA=small interfering RNA. *$p<0.01$ vs. control; †$p<0.01$ vs. IGF-1.

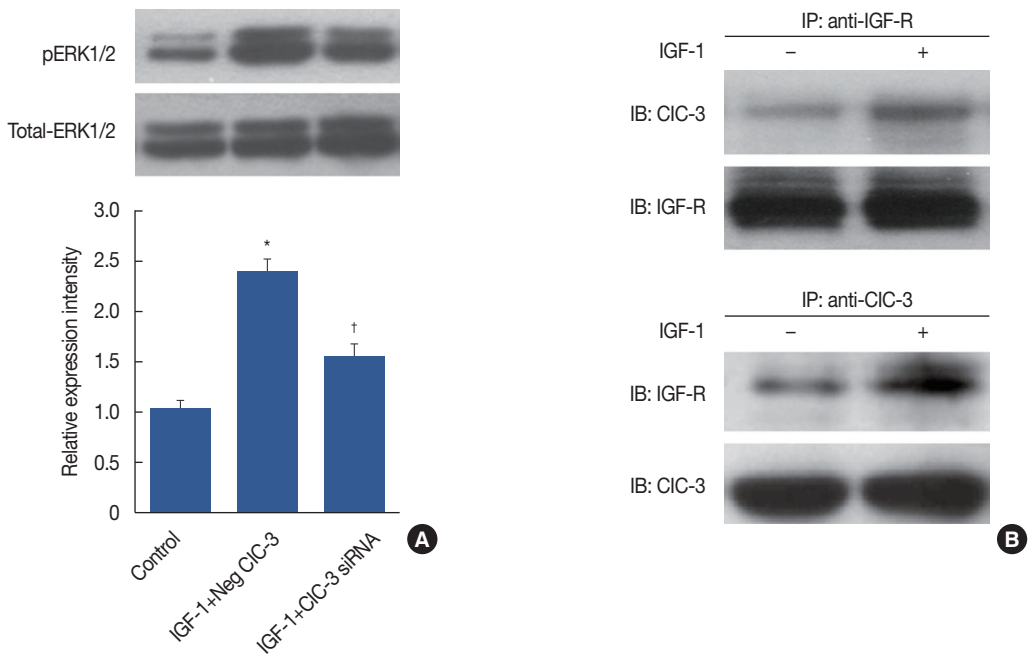

Figure 5. Effect of insulin-like growth factor 1 (IGF-1) induced extracellular regulated protein kinases 1/2 (ERK1/2) activation and the signal-responsive interaction of chloride channel-3 (ClC-3) with insulin-like growth factor receptor (IGF-R). (A) Effects of ClC-3 knockdown on the expression of ERK1/2 and phosphorylated ERK1/2 (pERK1/2). Bars represent mean±SD (n=5). Analysis of variance was employed for comparison. (B) Co-immunoprecipitation assay of ClC-3/IGF-R interaction in MDA-MB-231 cells (n=5). Cells were treated with or without IGF-1 (100 ng/mL). Protein extracts were immunoprecipitated (IP) with anti-IGF-R or anti-ClC-3 antibody, followed by immunoblotting (IB) with anti-IGF-R or anti-ClC-3.
siRNA=small interfering RNA. *$p<0.01$ vs. control; †$p<0.01$ vs. IGF-1+Neg ClC-3.

https://doi.org/10.4048/jbc.2018.21.2.103

stand how ERK1/2 activation was enhanced, we asked whether ClC-3 forms a signaling complex and functionally activates IGF-R. Interestingly, co-IP showed that ClC-3 interacted with IGF-R upon IGF-1 stimulation, in contrast to the control group (Figure 5B). Consequently, it markedly elevated the expression of ClC-3 and the signal-responsive ClC-3/IGF-R coupling was greatly facilitated, enhancing the activation of ERK1/2.

Knockdown of ClC-3 inhibits tumor growth in the xenograft carcinoma mouse model

As previously mentioned, ClC-3 is expressed in breast cancer. However, it is not clear whether suppression of ClC-3 alone can significantly affect tumorigenesis. Therefore, we transiently transfected MDA-MB-231 cells with either ClC-3 shRNA or negative control and injected them into the flanks of female nude mice. The outcome is of considerable interest, since we found that tumors derived from the MDA-MB-231 cells transfected with ClC-3 shRNA grew substantially slower compared to the negative control group during the entire tumor growth period. As shown in Figure 6A and 6B, the ClC-3 shRNA markedly inhibited tumor growth on days >18 ($p<0.01$). Immunostaining with anti-Ki-67 (Figure 6C) and western blot with anti-Ki-67, anti-PCNA, anti-cyclin D1, anti-cyclin E, and anti-pERK1/2 indicated that ClC-3 shRNA reduced tumor growth by inhibiting proliferation (Figure 6D). This was evident because the Ki-67 staining and cell cycle protein expression were much lower in the ClC-3 shRNA-treated cells than in the negative control.

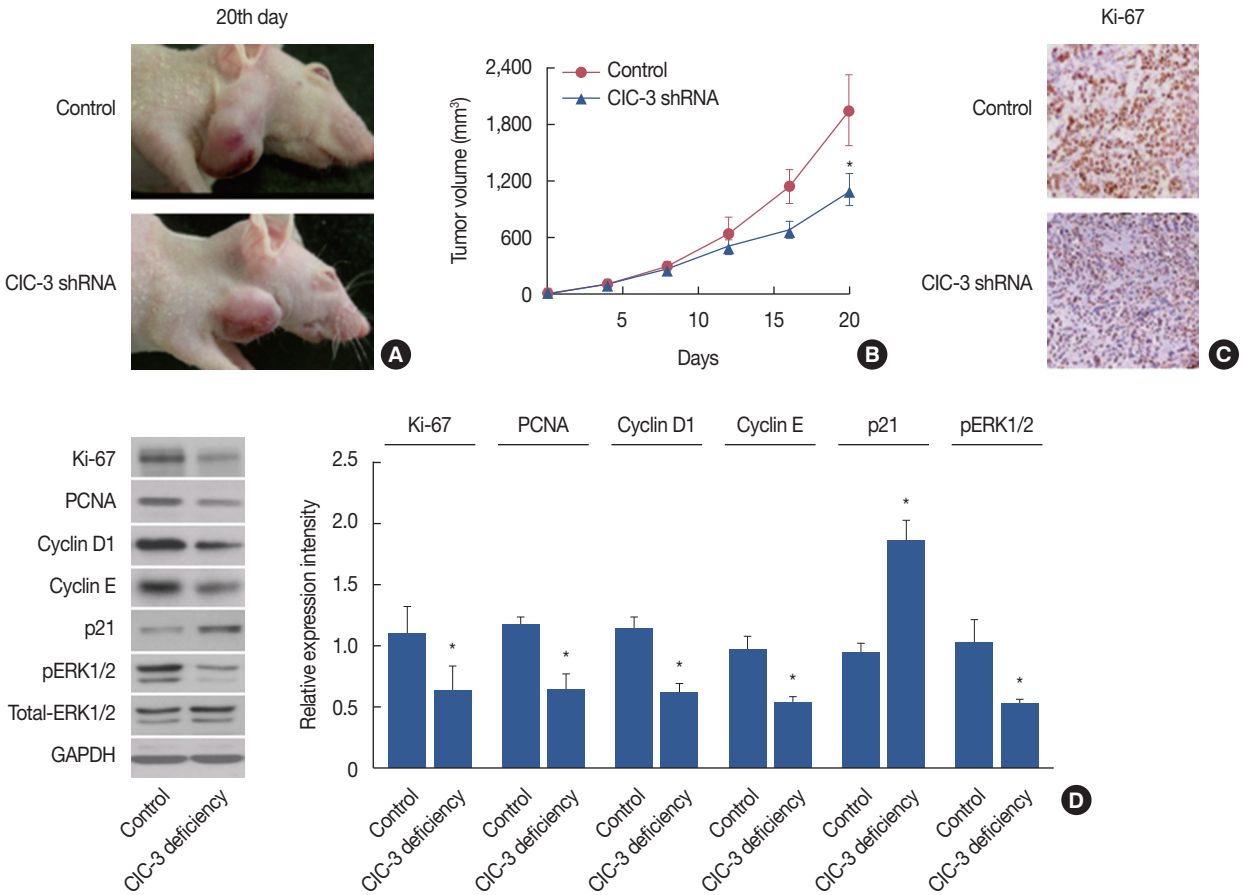

Figure 6. Effects of chloride channel-3 (ClC-3) knockdown on the growth of human breast tumors *in vivo*. (A) Representative images of tumors on day 20 from the control and ClC-3 short hairpin RNA (shRNA) groups. (B) Changes in tumor volume were calculated postinoculation every 4 days. Dots represent mean±SD. Seven mice were included in each group. Analysis of variance was employed for comparison. (C) Immunohistochemistry was performed to assess the expression of Ki-67 in tumor tissues isolated from control and ClC-3 shRNA mice, tumor tissues were cut and stained with hematoxylin-eosin, and observed with phase contrast microscope (×200). (D) Western blot analysis was performed to measure the expression of Ki-67, proliferating cell nuclear antigen (PCNA), cyclin D1, cyclin E, and phosphorylated extracellular regulated protein kinases1/2 (pERK1/2); glyceraldehyde 3-phosphate dehydrogenase (GADPH) was used as loading control (n=7).
*$p<0.01$ vs. control.

DISCUSSION

The present study describes the anticancer activity of ClC-3 knockdown in cultured breast cancer cells and in tumor xenograft animal models. *In vitro* experiments demonstrated that knockdown of ClC-3 inhibited proliferation in the human breast cancer cell line MDA-MB-231, arresting the cell cycle in the G_0/G_1 phase.

To further explore how ClC-3 is involved in human breast cancer cell proliferation, we observed the effects of ClC-3 knockdown in the cell cycle of MDA-MB-231 cells. Results indicated that knockdown of ClC-3 expression arrested the cell cycle in the G_0/G_1 phase in MDA-MB-231 cells. The well-orchestrated cell cycle regulatory proteins govern cell cycle progression [17]. These proteins include cyclins and CDK inhibitors (CDKIs) [18]. The activities of cyclin/cyclin-dependent kinase complexes can be inhibited by CDKIs. In this study, we investigated the expression of the regulatory proteins, and it was found that knockdown of the expression of ClC-3 downregulated the expression of cyclin D1 and cyclin E while increasing the level of p21 and CDKIs, which induce G_0/G_1 cell cycle arrest through inhibition of the cyclin/cyclin-dependent kinase complexes [19]. All obtained results demonstrated that knockdown of ClC-3 inhibited the proliferation of human breast cancer cells, which is likely explained by the restriction of G_0/G_1 to S phase transition during the cell cycle. This blockage is correlated with the ClC-3 shRNA-mediated downregulation of cyclins and upregulation of p21.

The mitogen-activated protein kinase (MAPK)/ERK pathway is a highly deregulated pathway in carcinogenesis and tumor progression [20]. In recent years, several currently available MAPK/ERK inhibitors have shown unprecedented clinical benefits in combating breast cancer [21]. The role of the MAPK/ERK signaling pathway in the proliferation, survival, motility, and differentiation of breast cancer cells has been recently reported [22]. Moreover, MAPK/ERK inhibitors were found to suppress the proliferation of breast cancer cells [23]. The present study associates ClC-3 expression and pERK1/2 with breast cancer progression, as ClC-3 protein expression was increased in breast cancer cells (MDA-MB-231). The human breast cancer cell line MDA-MB-231 is highly aggressive and migratory, as shown in previously published studies as well as in our study [15].

The high levels of pERK1/2 were strikingly associated with poor prognosis in breast cancer, based on poor differentiation, larger tumor sizes, and an advanced stage of breast cancer. The transient ClC-3 knockdown using shRNA markedly decreased the levels of pERK1/2 in MDA-MB-231 cells. This would suggest that ClC-3 may regulate pERK1/2. Over the past decade, ClC-3 was found to be expressed in human breast cancer, cervical cancer, prostate cancer, nasopharyngeal cancer, osteosarcoma, leukemia, and malignant glioma [3,10]. Several groups have reported that ClC-3 may regulate tumor cell proliferation, apoptosis, autophagy, cell cycle, migration, and invasion. The present study suggests that ClC-3 plays a key role in tumor proliferation and the cell cycle. Knockdown of ClC-3 inhibited tumor growth in our mouse xenograft model of breast carcinoma. Together, the results suggest that ClC-3 may directly affect the clinical outcome of breast cancer patients.

Taken together, we found that ClC-3 acts on the ERK1/2 signal transduction pathway to inhibit the progression of breast cancer. Nevertheless, further studies are needed to verify whether the knockdown of ClC-3 exerts effects other than the inhibition of proliferation, which could account for its antitumor activity. Our data could support the development of a novel treatment for human breast cancer that targets ClC-3.

CONFLICT OF INTEREST

The authors declare that they have no competing interests.

REFERENCES

1. Singh E, Joffe M, Cubasch H, Ruff P, Norris SA, Pisa PT. Breast cancer trends differ by ethnicity: a report from the South African National Cancer Registry (1994-2009). Eur J Public Health 2017;27:173-8.
2. Kreiter E, Richardson A, Potter J, Yasui Y. Breast cancer: trends in international incidence in men and women. Br J Cancer 2014;110:1891-7.
3. Yang H, Ma L, Wang Y, Zuo W, Li B, Yang Y, et al. Activation of ClC-3 chloride channel by 17beta-estradiol relies on the estrogen receptor alpha expression in breast cancer. J Cell Physiol 2018;233:1071-81.
4. Xu B, Jin X, Min L, Li Q, Deng L, Wu H, et al. Chloride channel-3 promotes tumor metastasis by regulating membrane ruffling and is associated with poor survival. Oncotarget 2015;6:2434-50.
5. Lemonnier L, Lazarenko R, Shuba Y, Thebault S, Roudbaraki M, Lepage G, et al. Alterations in the regulatory volume decrease (RVD) and swelling-activated Cl- current associated with neuroendocrine differentiation of prostate cancer epithelial cells. Endocr Relat Cancer 2005;12:335-49.
6. Mao J, Chen L, Xu B, Wang L, Li H, Guo J, et al. Suppression of ClC-3 channel expression reduces migration of nasopharyngeal carcinoma cells. Biochem Pharmacol 2008;75:1706-16.
7. Du S, Yang L. ClC-3 chloride channel modulates the proliferation and migration of osteosarcoma cells via AKT/GSK3beta signaling pathway. Int J Clin Exp Pathol 2015;8:1622-30.
8. Kasinathan RS, Föller M, Lang C, Koka S, Lang F, Huber SM. Oxidation induces ClC-3-dependent anion channels in human leukaemia cells. FEBS Lett 2007;581:5407-12.
9. Cuddapah VA, Sontheimer H. Molecular interaction and functional regulation of ClC-3 by Ca2+/calmodulin-dependent protein kinase II

 https://doi.org/10.4048/jbc.2018.21.2.103

(CaMKII) in human malignant glioma. J Biol Chem 2010;285:11188-96.
10. Hong S, Bi M, Wang L, Kang Z, Ling L, Zhao C. CLC-3 channels in cancer (review). Oncol Rep 2015;33:507-14.
11. Wang L, Ma W, Zhu L, Ye D, Li Y, Liu S, et al. ClC-3 is a candidate of the channel proteins mediating acid-activated chloride currents in nasopharyngeal carcinoma cells. Am J Physiol Cell Physiol 2012;303:C14-23.
12. Tang YB, Liu YJ, Zhou JG, Wang GL, Qiu QY, Guan YY. Silence of ClC-3 chloride channel inhibits cell proliferation and the cell cycle via G/S phase arrest in rat basilar arterial smooth muscle cells. Cell Prolif 2008;41:775-85.
13. Mao J, Chen L, Xu B, Wang L, Wang W, Li M, et al. Volume-activated chloride channels contribute to cell-cycle-dependent regulation of HeLa cell migration. Biochem Pharmacol 2009;77:159-68.
14. Huang YY, Huang XQ, Zhao LY, Sun FY, Chen WL, Du JY, et al. ClC-3 deficiency protects preadipocytes against apoptosis induced by palmitate in vitro and in type 2 diabetes mice. Apoptosis 2014;19:1559-70.
15. Huang EW, Xue SJ, Zhang Z, Zhou JG, Guan YY, Tang YB. Vinpocetine inhibits breast cancer cells growth in vitro and in vivo. Apoptosis 2012;17:1120-30.
16. Wang M, Tang YB, Ma MM, Chen JH, Hu CP, Zhao SP, et al. TRPC3 channel confers cerebrovascular remodelling during hypertension via transactivation of EGF receptor signalling. Cardiovasc Res 2016;109:34-43.
17. Malumbres M, Barbacid M. Cell cycle, CDKs and cancer: a changing paradigm. Nat Rev Cancer 2009;9:153-66.
18. Braun-Dullaeus RC, Mann MJ, Dzau VJ. Cell cycle progression: new therapeutic target for vascular proliferative disease. Circulation 1998;98:82-9.
19. Abbas T, Dutta A. p21 in cancer: intricate networks and multiple activities. Nat Rev Cancer 2009;9:400-14.
20. Dhillon AS, Hagan S, Rath O, Kolch W. MAP kinase signalling pathways in cancer. Oncogene 2007;26:3279-90.
21. Roberts PJ, Der CJ. Targeting the Raf-MEK-ERK mitogen-activated protein kinase cascade for the treatment of cancer. Oncogene 2007;26:3291-310.
22. Saini KS, Loi S, de Azambuja E, Metzger-Filho O, Saini ML, Ignatiadis M, et al. Targeting the PI3K/AKT/mTOR and Raf/MEK/ERK pathways in the treatment of breast cancer. Cancer Treat Rev 2013;39:935-46.
23. Mester J, Redeuilh G. Proliferation of breast cancer cells: regulation, mediators, targets for therapy. Anticancer Agents Med Chem 2008;8:872-85.